Journal of the Korean Nuclear Society
Volume 36, Number 5, pp. 403 414, October, 2004

Heat Transfer Characteristics of an Internally-Heated Annulus Cooled with R-134a Near the Critical Pressure

Sung-Deok Hong, Se-Young Chun, Se-Yun Kim, and Won-Pil Baek
Korea Atomic Energy Research Institute
150 Deokjin-dong, Yuseong-gu, Daejeon, Korea, 305-353
sychun@kaeri.re.kr

(Received March 23, 2004)

Abstract

An experimental study of heat transfer characteristics near the critical pressure has been performed with an internally-heated vertical annular channel cooled by R-134a fluid. Two series of tests have been completed: (a) steady-state critical heat flux (CHF) tests, and (b) heat transfer tests for pressure reduction transients through the critical pressure. In the present experimental range, the steady-state CHF decreases with increase of the system pressure for fixed inlet mass flux and subcooling. The CHF falls sharply at about 3.8 MPa and shows a trend towards converging to zero as the pressure approaches the critical point of 4.059 MPa. The CHF phenomenon near the critical pressure does not lead to an abrupt temperature rise of the heated wall, because the CHF occurs at remarkably low power levels. In the pressure reduction transients, as soon as the pressure passes below the critical pressure from the supercritical pressure, the wall temperatures rise rapidly up to very high values due to the departure from nucleate boiling. The wall temperature reaches a maximum at the saturation point of the outlet temperature, and then tends to decrease gradually.

Key Words : Supercritical pressure water reactor, Critical pressure, Critical heat flux, Heat transfer, Pressure transient, Annulus, R-134a

1. Introduction

Several supercritical-pressure light water reactor (SCWR) concepts have been investigated for the next generation nuclear reactors by a number of research institutes [1, 2]. SCWRs, which are operated above the thermodynamic critical point of water (647 K, 22.1 MPa), have advantages over conventional light water reactors (LWRs) in terms of thermal efficiency as well as in compactness and simplicity. SCWR plants adopt a once-through direct power conversion cycle similar to that of supercritical fossil fire power plants (FPPs). The coolant flow rate through the reactor core is about 1/10th that of conventional LWRs of equivalent thermal power.

In LWRs, critical heat flux (CHF) is an important thermal hydraulic parameter that limits the available power. Meanwhile, there is no criterion similar to the minimum CHF ratio (which is defined as a minimum of the ratio of CHF divided by the local heat flux) during normal operating conditions of SCWRs, because of the absence of phase change in the supercritical pressure conditions. However, fluids near to the thermodynamic critical point have the special characteristic that their thermodynamic properties vary rapidly with temperature and pressure. In the supercritical pressure region, the specific heat rises sharply and then falls steeply with fluid temperature for fixed pressure. The temperature at which the specific heat reaches its peak value is known as the pseudo-critical temperature. All the other thermodynamic properties vary strongly in the vicinity of the pseudo-critical temperature. Heat transfer to fluid at supercritical pressures is characterized by such variations of the thermodynamic properties with temperature. Near the pseudo-critical condition, an excessive increase in heat flux and/or a decrease in coolant flow rate can cause "heat transfer deterioration" [3]. When a SCWR is operated with a sliding pressure start-up scheme (i.e., the nuclear heating starts at sub-critical pressure), the CHF should be avoided during the power-increasing phase under sub-critical pressure conditions. Moreover, in order to ensure the reliability of safety analyses with the computer codes for abnormal transients including loss of coolant accidents, it is necessary to understand the heat transfer behavior during pressure transients from supercritical to sub-critical pressure regions [4].

Since the 1960s, many experimental studies have been performed on heat transfer in the boiler tubes of supercritical FPPs[3]. These efforts will be fully utilized for the development of SCWRs. However, the thermal-hydraulic conditions of the SCWR core are different from those of the FPP boiler, where heat is transferred from the tube wall to the supercritical water flowing inside tubes. In the SCWR core, the heat transfer to the supercritical fluid occurs on the outside surface of fuel rods in rod bundles with spacers. In addition, the hydraulic diameter of the SCWR core is much smaller than that of the boiler tube of the FPP.

The core design of a SCWR requires a stricter thermal-hydraulic analysis than that for an FPP boiler in order to ensure integrity and safety. Extensive CHF analyses have been conducted for the design of LWRs. Consequently, most of the existing CHF correlations are applied for the pressure and flow rate conditions corresponding to the normal operating ranges of LWRs. Only a few studies of the CHF near the critical pressure (Pr > 0.90) have been reported [5].

Experimental studies on heat transfer near the critical pressure with a single heater rod or rod bundles have yet to be carried out thus far, whereas considerable work has been done on heat transfer in the boiler tubes of supercritical FPPs. Therefore, the experimental study has been performed on steady-state CHF under sub-critical pressure conditions near the critical point and heat transfer during transition from the supercritical to sub-critical pressures with an internally-heated annulus cooled by R-134a (HFC134a) fluid. In this paper, the results from these experiments are presented and the heat transfer characteristics near the critical pressure are discussed.

2. Experiments

2.1. Experimental Loop

The experimental work has been performed in the Freon Thermal-Hydraulic Experimental Loop at the Korea Atomic Energy Research Institute (KAERI). This loop uses R-134a (P_c = 4.059 MPa,

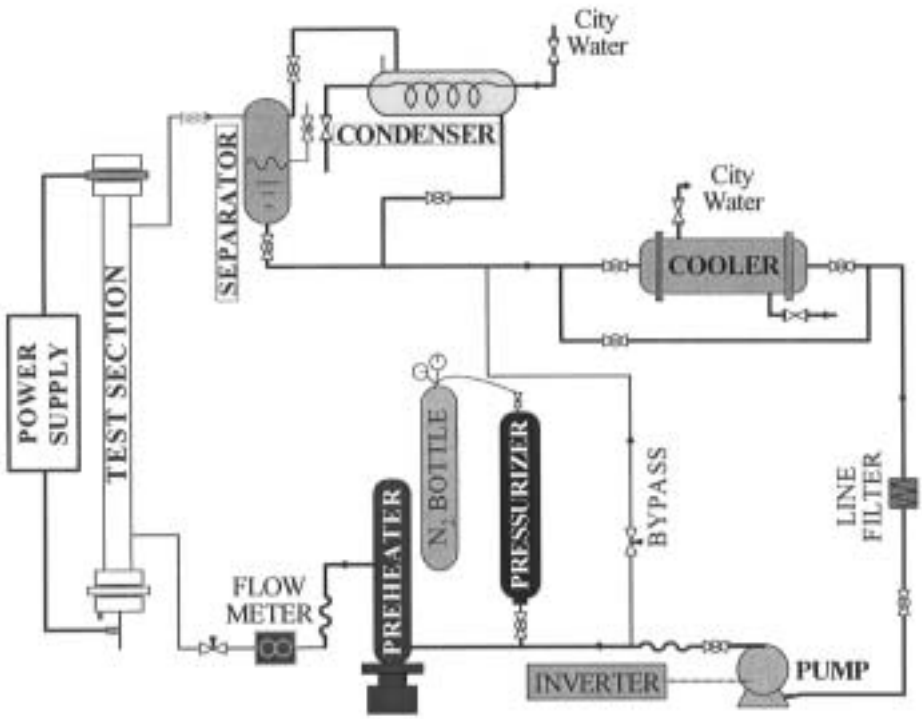

Fig. 1. Schematic Flow Diagram of Freon (R-134a) Experimental Loop

T_c = 374.2 K) as a working fluid and can be operated up to 4.50 MPa (water equivalent pressure, which is determined from the same reduced pressure, is 24.49 MPa.) and 423 K.

Figure 1 shows a simplified flow diagram of the Freon loop, which basically consists of a circulating pump, a preheater, a pressurizer, a test section, a vapor/liquid separator, a condenser, and a cooler. R-134a fluid is circulated in the main loop by a canned motor centrifugal pump. The flow rate through the test section inlet is controlled by adjustment of the circulating pump motor speed, the flow control valve, and the bypass valve. The inlet flow rate is measured by a Coriolis type mass flow meter. A throttling valve located at the upstream of the test section inlet is used to avoid flow fluctuation, which is usually observed under low flow rate conditions. The preheater adjusts the degree of subcooling of the fluid entering the test section. The two-phase flow mixture from the test section is separated into vapor and liquid in the separator. The separated vapor is condensed while flowing through a condenser attached to the separator. An accumulator-type pressurizer is used to control the loop pressure. The power to the test section is supplied from a 50 V x 800 A DC source. Protection of the test section heater rod against excessive temperature is provided by an automatic power run down/trip system that is operated by the CHF detection and protection system.

2.2. Test Section

Figure 2 shows details of the test section used in this experiment. An internally heated annular

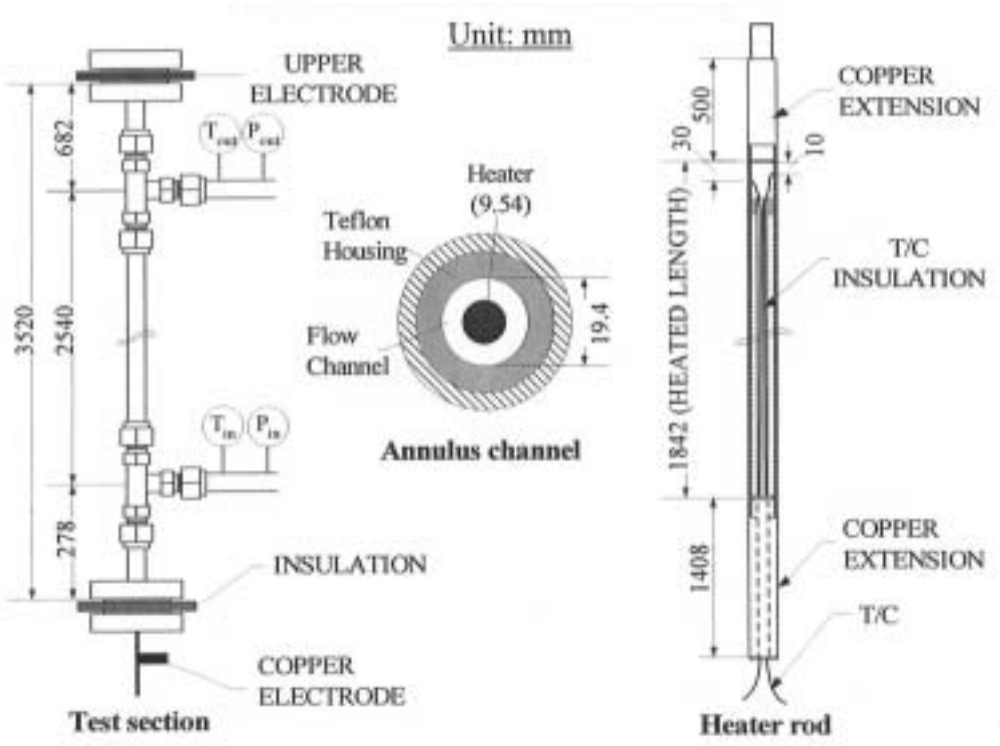

Fig. 2. Annulus Test Section Details

channel (inner diameter of 9.54 mm, outer diameter of 19.4 mm, and heated length of 1842 mm at room temperature) was used with vertical upward flow. The inner heater rod is made of Inconel 601 tube and directly heated by a large DC current passing through the heater wall. For measuring the heater rod wall temperatures and detecting the CHF occurrence, two K-type thermocouples with a sheath outer diameter of 0.5 mm are attached to the inside surface of the heater rod wall. The temperature sensing points of these thermocouples are located at 10 and 30 mm from the top end of the heated section.

2.3. Experimental Procedure and Conditions

Two series of tests have been conducted: a steady-state CHF experiment and a pressure-transient heat transfer experiment. In the CHF experiment, the flow rate, inlet subcooling, and system pressure (at the test section outlet) are first set to the desired levels. Power is then applied to the heater rod of the test section and increased gradually in small steps while the test section inlet conditions are kept constant. The CHF condition is defined as a sharp and continuous rise of the wall temperatures on the heater rod. The CHF detection and protection system continuously scans the temperature signals from the two thermocouples. When the wall temperature reaches a pre-determined set point, the DC power to the heater rod is automatically decreased or tripped by the power run down/trip system. The experimental conditions of the steady-state CHF experiment are as follows:

- system pressure : 0.63 ~ 3.98 MPa
  (water equivalent pressure: 4.03 ~ 21.71 MPa)
- mass flux : 501, 1002 and 1502 kg/m^{2}s

- inlet subcooling : 14.5, 24.8, 34.5 and 44.3 K

The water equivalent pressures are determined from the same liquid-to-vapor density ratio for the sub-critical region and from the same reduced pressure for the supercritical region.

In the pressure-transient heat transfer experiment, after the flow rate and inlet subcooling are established at desired levels, the system pressure (at the test section outlet) and the power to the heated section are gradually raised to establish initial conditions. In this study, the power was fixed at approximately two times that of the steady-state CHF values obtained at a pressure of 3.98 MPa (Pr=0.98), and the pressure transients were started when the system pressure reached about 4.14 MPa (Pr=1.02). The power was increased carefully in order to preclude the occurrence of CHF in the sub-critical pressure region. The system pressure was reduced from the supercritical pressure (at about 4.14 MPa) to the sub-critical pressure by releasing the nitrogen gas in the accumulator to the atmosphere. The flow rate, inlet subcooling, and the power to the heated section were kept constant during the pressure transient. The experimental conditions of the pressure transient experiments are listed in Table 1.

2.4. Measurement Uncertainties

The main parameters measured in the present experiments are fluid temperatures and pressures at the inlet and outlet of the test section, the temperatures of the heater rod, the flow rate, and the power applied to the heater rod. For performance of the experiments and analysis of the experimental data, the thermodynamic properties of R-134a from NIST Chemistry WebBook are used [6]. The uncertainties of the measuring system are estimated from calibration of the sensors and the accuracy of the equipment, according to a propagation error analysis based on Taylor's series method [7]. The evaluated maximum uncertainties of the pressures, flow rates, and temperatures are less than $\pm$0.3 %, $\pm$ 0.3 %, and $\pm$0.7 K of the readings in the range of interest, respectively. The uncertainty of the heat flux calculated from the applied power is always less than $\pm$1.8% of the readings. The heat loss in the test section is taken into account in the calculation of heat flux. Before starting a set of experiments, pretests (i.e., heat balance tests) were carried out to estimate the heat loss from the test section. The heat losses estimated by the pretests for each pressure condition are less than 1.0% of the power input.

3. Experimental Results and Discussions

3.1. Steady-state CHF tests

Regarding influence of the system pressure on the CHF at fixed inlet subcooling conditions, Collier and Thome [8] predicted that the CHF for water flow in a tube would pass through a maximum in the low pressure range (below 3 MPa) and then decrease monotonously as the pressure increases, and that a second maximum would be found in the high pressure range of 10 ~ 20 MPa. Two peaks of CHF with pressure were observed experimentally by Yin et al. [5]. They reported that with water in a tube for fixed inlet subcooling conditions a second peak of CHF appears around 19.0 MPa.

Figure 3 shows the CHFs for R-134a fluid. They were measured in a pressure range of 0.63 ~ 3.98 MPa for a fixed inlet subcooling ΔT_{sub} of 14.5 K, with the mass flux as a parameter. A second CHF peak is not evident in this figure. However, the slopes of the CHF curve become smaller between 2.0 and 3.7 MPa. This indicates the possible existence of a second peak on the CHF curve for other conditions.

Figure 4 shows the CHF for R-134a fluid as a function of pressure with the inlet subcooling as a parameter. As can be seen from Figs. 3 and 4, the CHF values fall sharply at about 3.8 MPa as the pressure approaches the critical value. The CHF values then show a trend towards converging to zero. Consequently, the effects of the mass flux and inlet subcooling on the CHF become smaller at a pressure of about 3.98 MPa. This trend was also observed in water experiments performed at a constant mass flux by Yin et al. [5]. The sharp decrease of the CHF above 3.8 MPa is magnified by increasing the inlet subcooling and the mass flux, as shown in Figs. 3 and 4. In the present study, the inlet subcooling is represented in terms of the subcooling temperature (i.e., $\Delta T_{sub} = T_{sat} - T_{in}$) instead of the inlet subcooling enthalpy or inlet quality frequently employed in the literature [9, 10]. If the inlet subcooling enthalpy is held constant, the inlet subcooling temperature decreases as the system pressure increases. Generally, the CHF decreases linearly with decreasing inlet subcooling for fixed pressure and mass flux conditions. Figure 4 shows that this relationship also holds up to a pressure of 3.98 MPa. Therefore, the conditions where the inlet subcooling enthalpy is held constant may accentuate the decrease of the CHF with an increase of pressure.

The sharp decrease of CHF near the critical pressure (above 3.8 MPa) is closely related to the thermodynamic properties of the R-134a fluid. Figure 5 shows the critical quality x_{CHF} for R-134a, which is the thermodynamic quality at the CHF occurrence location, together with the latent heat of vaporization h_{lg}, saturated liquid and vapor densities ρ and specific heat of the saturated liquid C_p as a function of pressure. In Fig. 5, the scale of the y-axis for the latent heat, densities, and specific heat is chosen arbitrarily. The values of critical quality show very little variation up to a pressure of 3.0 MPa and then decrease slowly as the pressure increases. When the pressure nears the critical point above 3.7 MPa, the thermodynamic properties start to change sharply

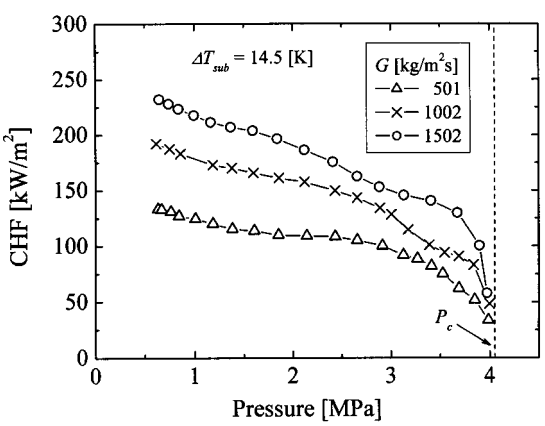

Fig. 3. CHF Trend for the System Pressure

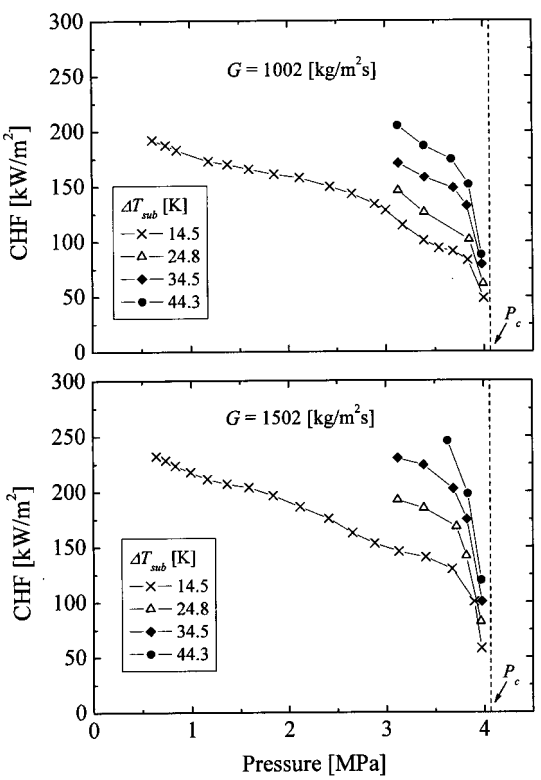

Fig. 4. The Effect of Inlet Subcooling on CHF Near the Critical Pressure

and the critical qualities decrease suddenly at this pressure. It is especially notable that the sharp decrease of the CHF and the latent heat (which becomes zero at the critical pressure) commences at almost the same pressure. It can be speculated that the sharp decrease of the CHF might be caused by the decrease of latent heat. In the pressure region where the thermodynamic properties vary sharply, the inlet conditions of the test section were adjusted very carefully, because a slight change of the conditions could lead to a relatively large change of the CHF value.

The general consensus is that for flow boiling the physical mechanism of the CHF can be classified as departure from nucleate boiling (DNB) or liquid film dryout. DNB occurs when the bulk liquid is subcooled or at low vapor quality and is characterized by a rapid rise in the heated wall temperature. Liquid film dryout occurs in annular flow or annular-mist flow under high vapor quality conditions, and the heated wall temperature rises comparatively slowly with its oscillations. In the present experiments, most of the critical qualities for the pressure conditions above 3.0 MPa have negative values except for a part of the data for the mass flux of 501 kg/m²s and the inlet subcooling of 14.5 K, as can be seen from Fig. 5. Figure 5 also shows that for pressures above 3.5 MPa the heat transfer from the heater rod surface to the fluid is due to subcooled boiling. Furthermore, the CHFs at a pressure of 3.98 MPa occur under very highly subcooled conditions, because the range of the critical qualities at 3.98 MPa is from -1.03 to -2.66. The wall temperature variations at a location of 30 mm from the top end of the heated section at CHF conditions for R-134a are shown in Fig. 6. According to the conventional view of CHF characteristics noted above, the temperature variation for the pressure of 0.66 MPa in Fig. 6(a) represents a typical dryout. On the other hand, the temperature variations for the pressures of 3.18 MPa in Fig. 6(a) and 3.13 MPa in Fig. 6(b) (water equivalent

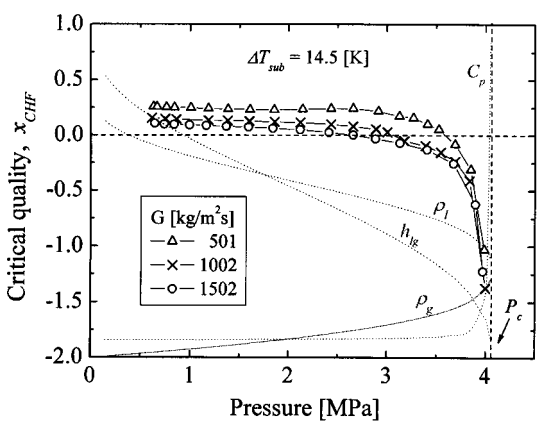

Fig. 5. Critical Quality and Thermodynami Properties with Pressure

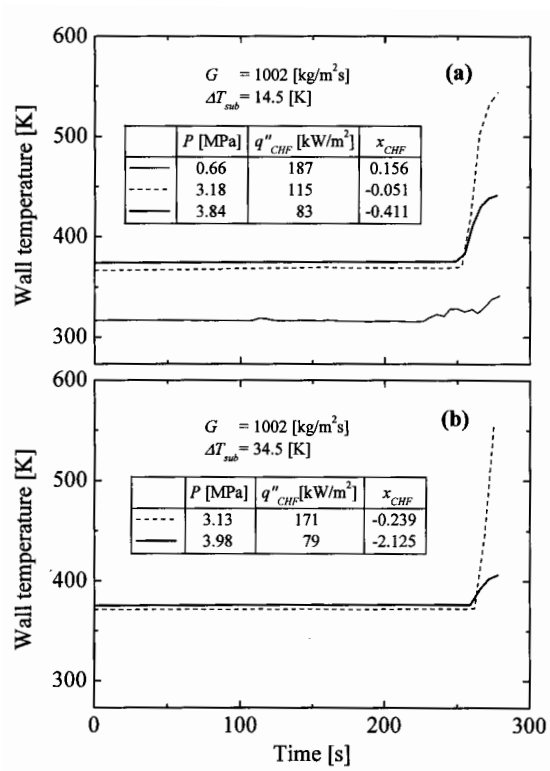

Fig. 6. Wall Temperature Variations of the Heater Rod at CHF Conditions

pressures are 18.03 and 17.79 MPa, respectively.) show typical DNB characteristics. At pressures near the critical point, that is, 3.84 MPa in Fig. 6(a) and 3.98 MPa in Fig. 6(b) (water equivalent pressures are 21.11 and 21.71 MPa, respectively), the features of the temperature variations are regarded as DNB because of the high subcooled conditions. However, the wall temperatures rise slowly, compared to the case of the DNB at normal pressure conditions below 3.18 MPa. This implies that the CHF phenomenon near the critical pressure no longer leads to an inordinate increase in the heated wall temperature, such as the case of DNB *at normal pressure conditions*, because the occurs at remarkably low power levels. The CHF phenomenon disappears at the critical pressure. The sharp and continuous rise of the wall temperature, which indicates CHF occurrence, will not be observed at the critical pressure since the latent heat and the density ratio ρ_f / ρ_g at saturation become zero and unity, respectively, as the pressure approaches the critical pressure.

3.2. Heat Transfer Tests During Pressure Transients

Table 1. The Conditions of the Pressure Transient Experiments

Parameter	Unit	Run1	Run2	Run3	Run4	Run5
Mass flux	kg/m^2s	500	982	1452	1475	1504
Heat flux	kW/m^2	69.6	110.0	126.3	169.9	239.0
CHF*	kW/m^2	33.5	48.4	58.0	82.0	119.5
T_{in}	K	359.5	359.9	360.1	350.2	329.2
T_{out}	K	371.6	369.8	367.2	363.7	351.5
$\Delta T_{\text{sub-initial}}$**	K	14.9	14.7	14.6	24.0	44.7
P_{initial}	MPa	4.12	4.14	4.17	4.16	4.13

Note * : Steady-state CHF at 3.98 MPa (Pr = 0.98)

** $\Delta T_{\text{sub-initial}} = T_c - T_{in}$

In the current conceptual designs of the SCWR, the coolant enters the reactor core at a temperature of 553 K and is heated up to temperatures above 773 K while passing through the core at a system operating pressure of 25 MPa [1, 2]. During abnormal pressure transients such as loss of coolant accidents, the specific volume of high temperature coolant above the critical point (647 K) increases continuously as the system pressure decreases from the supercritical to sub-critical regions. In this case, the process of heat transfer is that of a single-phase liquid-like or gas-like fluid, and superheated vapor. On the other hand, the thermal-hydraulic behavior of the coolant below the critical temperature may show complicated features, because the liquid-vapor phase change begins when the pressure reaches the saturation point. Therefore, the pressure transient experiments with an internally-heated annulus cooled by R-134a fluid were carried out under flow conditions at which the fluid temperatures at the outlet from the test section were below the critical temperature, as shown in Table 1.

The wall temperature behavior at a location of 30 mm from the top end of the heated section of the heater rod was observed during the pressure transients from the supercritical to the sub-critical regions, as shown in Figs. 7 ~ 11. The variations of the outlet fluid temperature of the test section, the saturation temperature, and the quality at the exit of the heated section are also shown in these figures. The pressure decrease starts at about 4.14 MPa due to nitrogen gas being exhausted from the accumulator. The pressure reducing ratio is adjusted by controlling the amount of exhausted nitrogen gas. The nitrogen gas is continuously released until an experimental run is over. During the pressure transients, the mass flux, the test section inlet fluid temperature, and the heat flux were held at constant values. The test section

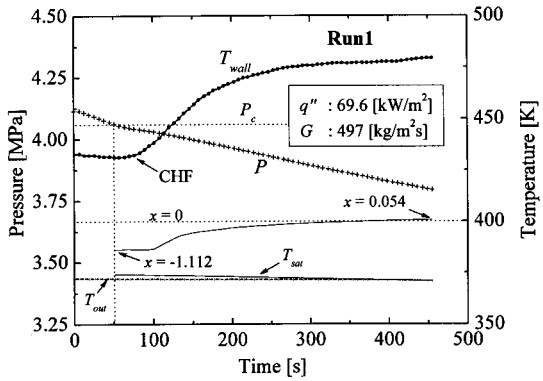

Fig. 7. Wall Temperature and Pressure Variations During Pressure Transient-Run 1

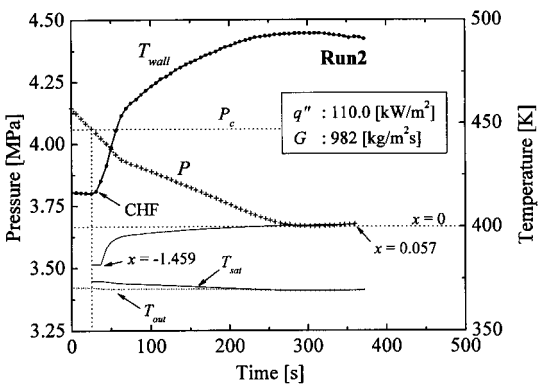

Fig. 8. Wall Temperature and Pressure Variations During Pressure Transient-Run 2

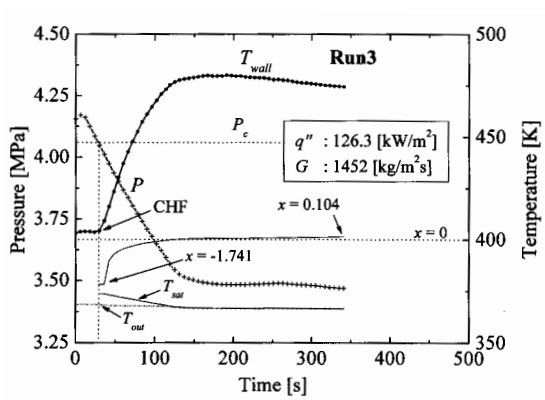

Fig. 9. Wall Temperature and Pressure Variations During Pressure Transient-Run 3

outlet fluid temperatures showed little variation with decreasing pressure.

In the supercritical pressure region, the wall temperatures scarcely vary with pressure, as shown in Figs. 7 ~ 11. As soon as the pressure passes through the critical pressure, the wall temperature rises suddenly. This phenomenon is regarded as the DNB in subcooled boiling, because the bulk fluid at the starting point of the wall temperature increase is strongly subcooled (below a quality of -1.11). In the previous section, it was noted that the CHF near the critical pressure no longer leads to an inordinate increase of the heated wall temperature. However, the wall temperatures rise rapidly up to a very high temperature in this experiment since the heat fluxes are set at high levels (about two times that of the values obtained at a pressure of 3.98 MPa).

If heat transfer in two-phase flow is classified as pre-CHF and post-CHF, the heat transfer of the post-CHF region after the CHF occurrence in Figs. 7 ~ 10 is due to inverted annular-flow film-boiling or dispersed flow film-boiling for $x < 1$ and a single phase flow of the superheated vapor for $x > 1$. It should be noted that film-boiling can occur at $x > 1$ because of non-equilibrium between the

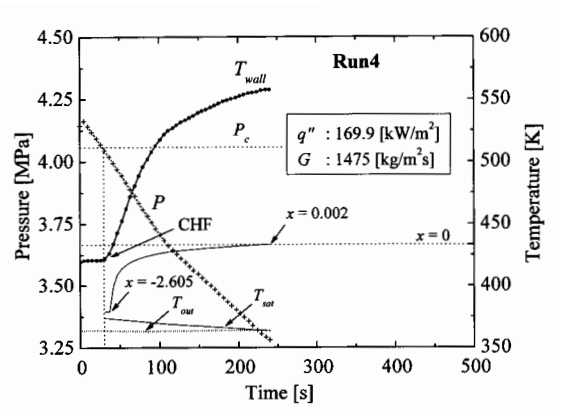

Fig. 10. Wall Temperature and Pressure Variations During Pressure Transient-Run 4

phases (i.e., liquid can still be present at $x > 1$). For the conditions of the present experiments, if the above consideration for *normal pressure conditions* is applicable, the heat transfer pattern in the post-CHF region may be mainly inverted annular-flow film-boiling, because the qualities are very low or negative ($x < 0.104$) during the pressure transients.

Figures 3 and 4 referred to in the previous section show that the steady-state CHF increases with decreasing pressure. This trend restrains the wall temperature increase and thus the slopes of the wall temperature increase become reduced with decreasing pressure, as shown in Figs. 7 ~ 10. The saturation temperature decreases with the decreasing pressure. Therefore, the saturation temperature approaches the fluid temperature of the test section outlet as the pressure decreases. In Figs. 8 and 9, after the saturation temperature coincides with the outlet temperature, the pressures do not decrease further, even though the nitrogen gas is continuously released in order to reduce the pressure. The reason why the pressure does not decrease further is because saturated film-boiling begins and flashing and evaporation occur actively at the outlet of the test section. When the CHF values for the region where the pressures scarcely decrease are roughly estimated from the steady state CHF data of Figs. 3 and 4, they are found to be slightly less than the heat fluxes of runs 2 and 3 in the transient experiments. In addition, a higher heat transfer is obtained for saturated film-boiling with active evaporation in the liquid core. Thus, the wall temperature value reaches a maximum at the point where the outlet fluid temperature becomes equal to the saturation temperature, and after that, the wall temperatures tend to decrease gradually (Figs. 8 and 9). In Fig. 7 for run 1, the wall temperature is seen to increase slightly and a clear maximum wall temperature is not observed since

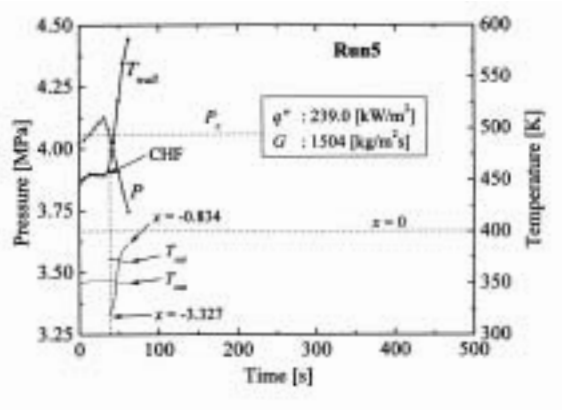

Fig. 11. Wall Temperature and Pressure Variations During Pressure Transient-Run 5

the pressure decreases slowly.

Figures 7 ~ 10 show that thermal equilibrium conditions hold steadily during the pressure transients under the present experimental conditions, because the points where the quality is equal to zero accord with the points where the outlet fluid temperature reaches the saturation value. In run 5 with the highest heat flux and very fast pressure transient (Fig. 11), the features of wall temperature behavior observed in the other runs are not found. The wall temperature rises abruptly to a high value the moment that the pressure passes through the critical pressure. In order to protect the heater rod from any damage, the power supply to the heater was cut off early in run 5.

4. Conclusions

Two series of experiments have been performed with an internally heated, vertical annular channel cooled by R-134a fluid: (a) steady-state CHF tests at sub-critical pressure conditions near the critical point, and (b) heat transfer tests during pressure decrease from supercritical to sub-critical pressures. The following conclusions can be drawn from this study:

(a) The steady-state CHF decreases with increase of the system pressure for fixed inlet mass flux

and subcooling. The CHF falls sharply at about 3.8 MPa and shows a trend towards converging to zero as the pressure approaches the critical point of 4.059 MPa.

(b) When the pressure approaches the critical pressure, the critical quality also drops very sharply and represents subcooled conditions.

(c) The CHF phenomenon near the critical pressure does not lead to an abrupt temperature rise of the heated wall because the CHF occurs at remarkably low power levels.

(d) In the pressure reduction transients, as soon as the pressure passes from above to below the critical pressure, the wall temperatures rise rapidly up to very high values due to the occurrence of departure from nucleate boiling.

(e) In the pressure reduction transients, the wall temperature reaches a maximum at the saturation point of the outlet temperature, and then tends to decrease gradually. This can be related to the trend of CHF increase with decreasing pressure.

Acknowledgements

This study has been carried out under the Nuclear R & D Program supported by the Ministry of Science and Technology (MOST) of Korea. The authors wish to express their appreciation to Mr. Y. J. Yoon and Mr. B. D. Kim for their help in performing the experiments.

Nomenclature

C_p	specific heat of saturated liquid [kJ/kgK]
G	mass flux [kg/m^{2}s]
h	enthalpy [kJ/kg]
hl_g	latent heat of vaporization [kJ/kg]
P	system pressure [MPa]
Pc	critical pressure [MPa]
Pr	reduced pressure, P/P_c [-]
q''	heat flux [kW/m^2]
T	fluid temperature [K]
ΔT_{sub}	inlet subcooling, T_{sat} - T_{in} [K]
x	thermodynamic quality at the exit of the heated section [-]
x_{CHF}	critical quality, that is, thermodynamic quality at CHF occurrence location [-]
ρ	density at saturation [kg/m^3]

Subscripts

c	critical condition
CHF	critical heat flux
g	vapor phase
in	test section inlet
l	liquid phase
out	test section outlet
r	reduced
sat	saturation
sub	subcooled
wall	wall of heater rod

Abbreviations

CHF	critical heat flux
DC	direct current
DNB	departure from nucleate boiling
FPP	fossil fire power plant
LWR	light water reactor
SCWR	supercritical - pressure light water cooled reactor
T/C	thermocouple

References

1. Y. Oka, "Research and development of the supercritical-pressure light water cooled reactors," Proceedings of the 10th International Topical Meeting on Nuclear Reactor Thermal Hydraulics (NURETH-10), Paper KL-02,Seoul,

Seoul, Korea (2003).

2. D. Squarer, T. Schulenberg, D. Struwe, Y.Oka, D. Bittermann, N. Aksan, C. Maraczy, R. Kyrki-Rajamaki, A. Souyri and P. Dumaz, "High performance light water reactor," Nucl Eng. Des., 221, pp. 167-180 (2003).
3. J. D. Jackson and W. B. Hall, "Forced convection heat transfer to fluids at super-critical pressure," Turbulent forced convection in channels and bundles (Edited by S. Kakac and D. B.Spalding), Hemisphere,Vol. 2, pp. 563-612 (1979).
4. P.. Dumaz and O. Antoni, "The extension of the CATHARE2 computer code above the critical point, applications to a supercritical light water reactor," Proceedings of the 10th International Topical Meeting on Nuclear Reactor Thermal Hydraulics (NURETH-10), Paper I00403, Seoul, Korea (2003).
5. S. T. Yin, T. J. Lui, Y. D. Huang and R. M. Tain, "Measurements of critical heat flux in forced flow at pressures up to the vicinity of the critical point of water," Proceeding of the 1988 National Heat Transfer Conference in U.S.A., Vol. 1, pp. 501-506, Houston (1988).
6. http://webbook.nist.gov/chemistry/, "NIST Standard Reference Database Number 69 - March, 2003 Release," (2003).
7. "ANSI/ASME PTC 19.1, ASME performance test codes, supplement on instruments and apparatus, part 1, measurement uncertainty," Published by ASME, New York (1985).
8. J. G. Collier and J. R. Thome, "Convective boiling and condensation, 3rd edition," Oxford University Press, pp. 361-363 (1994).
9. Se-Young Chun, Heung-June Chung, Sung-Deok Hong, Sun-Kyu Yang and Moon-Ki Chung, "Critical heat flux in uniformly heated vertical annulus under a wide range of pressures-0.57 to 15.0 MPa," Journal of the Korean Nuclear Society, 32[2], pp. 128-141 (2000).
10. I. L. Pioro, D. C. Groeneveld, L. K. H. Leung, S. S. Doerffer, S. C. Cheng, Yu. V. Antoshko, Y. Guo and A. Vasic, "Comparison of CHF measurements in horizontal and vertical tubes cooled with R-134a," Int. J. Heat Mass Transfer, 45, pp. 4435-4450 (2002).